PHYSICAL REVIEW E **72**, 055202(R) (2005)

Stable stationary and breathing holes at the onset of a weakly inverted instability

Orazio Descalzi[1,2] and Helmut R. Brand[2]
[1]*Facultad de Ingeniería, Universidad de los Andes, Santiago, Chile*
[2]*Department of Physics, University of Bayreuth, 95440 Bayreuth, Germany*
(Received 15 July 2005; published 28 November 2005)

We show numerically different stable localized structures including stationary holes, moving holes, breathing holes, stationary and moving pulses in the one-dimensional subcritical complex Ginzburg–Landau equation with periodic boundary conditions, and using two classes of initial conditions. The coexistence between different types of stable solutions is summarized in a phase diagram. Stable breathing moving holes as well as breathing nonmoving holes have not been described before for dissipative pattern-forming systems including reaction-diffusion systems.

DOI: 10.1103/PhysRevE.72.055202 PACS number(s): 82.40.Ck, 82.40.Bj, 05.70.Ln

The observation of localized structures in dissipative systems [1] in a number of fields has attracted growing attention. This field got a big boost by the experimental observation of localized propagating structures in a surface reaction [2] and self-replicating spots in a bulk chemical reaction [3]. The latter phenomenon has been discussed theoretically, in particular, in the framework of reaction-diffusion systems [4,5]. One has also observed oscillating localized states ("oscillons") in granular media [6] and two-dimensional (2D) localized structures in a laser with a saturable absorber [7] following a theoretical prediction [8].

To model such phenomena there have been two avenues of approach. Either reaction-diffusion models are studied, which were thought to be close to the autocatalytic chemical reactions investigated experimentally [4,5,9–12], or one investigates envelope equations [13,14], which reflect the symmetry of the underlying problem. In the domain of the envelope equations, the cubic complex Ginzburg–Landau (CGL) equation is very popular and shows many interesting phenomena including spatiotemporal chaos, but is not suitable to describe stable localized solutions [15]. Thual and Fauve showed [16] that a quintic complex Ginzburg–Landau equation with a destabilizing cubic term gives rise to stable localized solutions. In the following this observation was generalized to show that periodically and chaotically breathing localized solutions [17], as well as propagating fixed shape localized solutions [18,19], also stably exist for the quintic CGL equation. The quintic CGL equation represents an important prototype equation, since it arises generically as an envelope equation for a weakly inverted bifurcation associated with traveling waves. It also applies to real systems, in particular, from nonlinear optics including ring fiber lasers (compare Ref. [20] and references therein).

Another large class of localized solutions familiar, for example, from nonlinear optics, are hole solutions. They have already been shown to exist for the cubic CGL equation [21,22], but are known to be unstable against small changes in the equations [15] (structural instability).

Motivated by recent work on the stable existence and even coexistence of π and 2π holes for the same parameter values in the equation for a simple reaction-diffusion system [23] (compare Ref. [24] for a discussion of its relation to the one-dimensional (1D) quintic CGL equation), we are describing here numerical results on localized solutions and five types of different holes for the 1D quintic CGL equation. The five types of stable holes are: nonmoving π holes, nonmoving 2π holes, moving π holes (moving to the left or to the right), breathing moving holes (moving to the left or to the right), and breathing nonmoving holes. While traveling breathing pulses have been reported for a 1D reaction-diffusion system [25], this type of solution has not yet been found for the quintic CGL equation. We also discuss to what extent there are regimes of stable coexistence of the various types of stable pulse and hole solutions. Since these results are obtained for a generic envelope equation, we expect that such behavior is applicable to many types of systems [26].

The starting point of our investigations is the subcritical complex Ginzburg–Landau equation with periodic boundary conditions

$$\partial_t A = \mu A + (\beta_r + i\beta_i)|A|^2 A + (\gamma_r + i\gamma_i)|A|^4 A + (D_r + iD_i)\partial_{xx} A, \tag{1}$$

where $A(x,t)=R(x,t)e^{i\phi(x,t)}$ is a complex field.

A numerical study of Eq. (1) has been carried out using the following parameter values: $\beta_r=-\gamma_r=D_r=1$, $\beta_i=0.2$, $\gamma_i=0.15$, and $D_i=-0.1$ [27]. Different localized solutions arise as a function of μ and the initial conditions. We use two classes of initial conditions: initial conditions in phase (ICP) and initial conditions in antiphase (ICA) (see Fig. 1). The former is obtained by using $\mathrm{Im}\,A(x)=0$ and localized $\mathrm{Re}\,A(x)$ positive (or negative) and the latter by choosing $\mathrm{Im}\,A(x)=0$ and $\mathrm{Re}\,A(x)$ with a positive and a negative part (compare Fig. 1). We note that none of the results presented

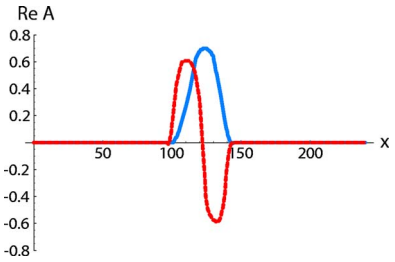

FIG. 1. (Color online) Generic localized initial conditions: in phase (ICP) shown as solid line and in antiphase (ICA) shown as dashed line.

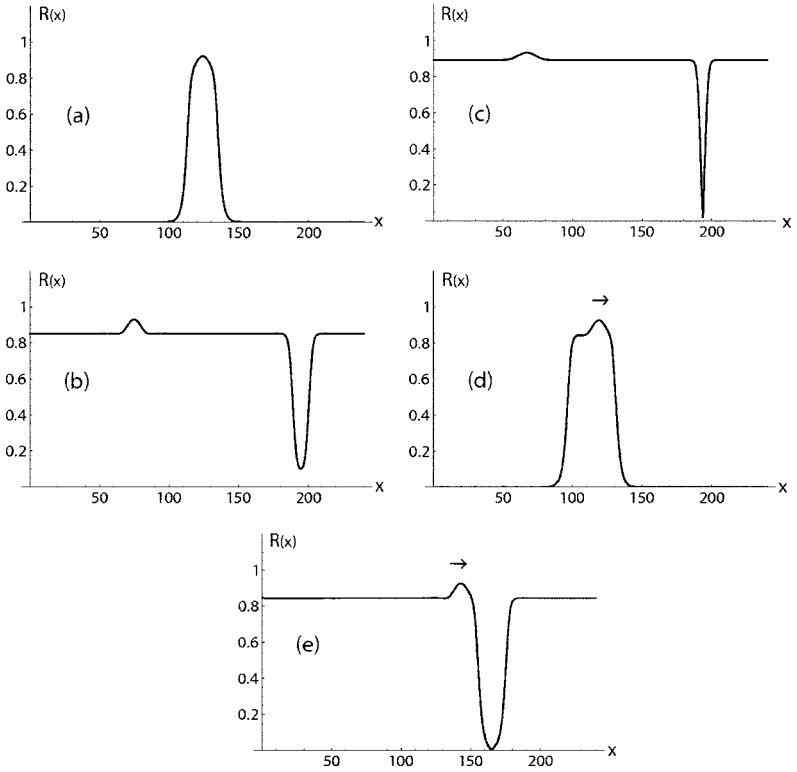

FIG. 2. The modulus R is shown for different stable localized structures. (a) Stationary pulse for $\mu=-0.1200$. (b) Stationary 2π hole for $\mu=-0.1080$. (c) Stationary π hole for $\mu=-0.1080$. (d) Right-moving pulse for $\mu=-0.1136$. (e) Right-moving hole for $\mu=-0.1133$.

below depends on the details of the shape of the initial conditions; for example, they do not need to be anywhere near a Gaussian in shape. As a numerical method we used fourth-order Runge–Kutta finite differencing. We used typically 600 points with $dx=0.4$ (corresponding to a box length of $L=240$) and a time step of $dt=0.1$. We were performing up to 10^6 iterations to check for long transients corresponding to a total time of $T=10^5$. We also changed dx and dt to verify that none of the results presented depends sensitively on the discretization used. We note that there is at maximum a small shift in the values of μ by at maximum 0.1% for which some of the solutions with a narrow range of stable existence arise.

The results for ICP are the following: For $\mu<-0.168\,97$ the system goes to zero. For $-0.168\,97<\mu<-0.1110$ we obtain stationary pulses [see Fig. 2(a)]. In the narrow range $-0.1110<\mu<-0.1107$ any ICP evolves to the homogeneous solution. For $-0.1107<\mu<-0.1045$ any ICP gives origin to a stationary 2π hole, whose modulus does not touch zero [see Fig. 2(b)]. In the very wide range $-0.1045<\mu<-0.088\,04$ any ICP reaches a stationary π hole, whose modulus touches zero [see Fig. 2(c)]. For $-0.088\,04<\mu<-0.088\,00$ appear chaotic holes. In the vicinity of $\mu=-0.088\,00$ we find that period doubling can precede the onset of chaotic behavior. In the range $-0.088\,00<\mu<-0.087\,93$ any ICP evolves either to a right- [see Figs. 3(a) and 3(b)] or left-moving breathing hole, which is asymmetric and whose modulus is not reaching zero. For $-0.087\,93<\mu<-0.087\,67$ the holes change to nonmoving breathing holes and they are symmetric [see Figs. 3(c) and 3(d)]. The x-t plots clearly show that the depicted breathing holes act as

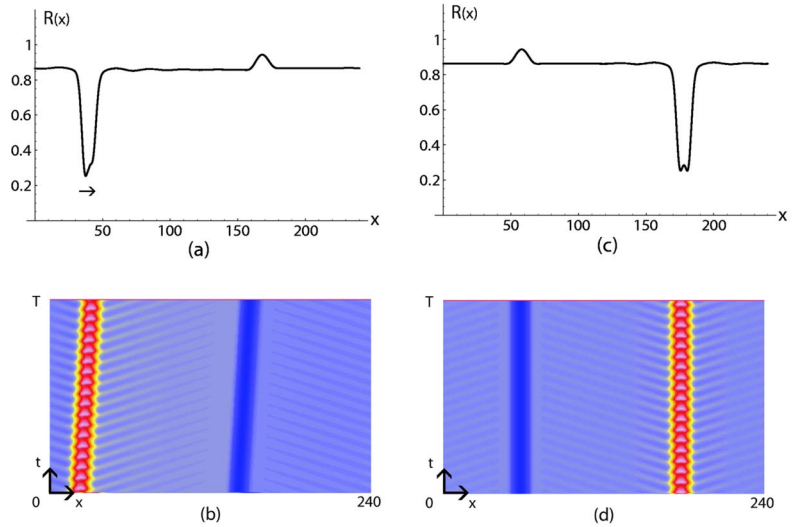

FIG. 3. (Color online) The modulus R and space-time plots for the modulus of breathing stable localized structures. (a) and (b) Breathing right-moving hole for $\mu=-0.087\,95$. (c) and (d) Breathing nonmoving hole for $\mu=-0.087\,80$. In the x-t plots (b) and (d) the time shown on the ordinate is $T=10^3$ corresponding to 10^4 iterations.

a sink of traveling waves in both cases. For $\mu > -0.087\,67$ the system evolves to the homogeneous solution.

There is no coexistence between chaotic, moving breathing, and nonmoving breathing holes.

The results for ICA are the following: For $\mu < -0.168\,97$ the systems goes to zero. For $-0.168\,97 < \mu < -0.113\,64$ we obtain stationary pulses. In the narrow range $-0.113\,64 < \mu < -0.113\,47$ any ICA evolves either to a right- [see Fig. 2(d)] or a left-moving pulse, which is asymmetric and has fixed shape. For $-0.113\,47 < \mu < -0.113\,18$ appear either right- [see Fig. 2(e)] or left-moving holes, which are asymmetric π holes and whose modulus reaches zero. For $-0.113\,18 < \mu < -0.1118$ the system evolves to the homogeneous solution. In the very narrow range $-0.1118 < \mu < -0.1110$ appear stationary 2π holes. In the very wide range $-0.1110 < \mu < 0$ any ICA reaches a stationary π hole. We have checked by varying the system size, that even solutions which exist only over a narrow range of μ persist in their stable existence. Only the precise location of the stable interval on the μ axis is shifted by a very small amount.

We remark that the homogeneous solutions near pulses (ICP or ICA) have a wave vector different from zero but the homogeneous solutions found for ICP near breathing holes have a vanishing wave vector. The humps observed in the stationary and moving holes correspond to sources of traveling waves. We point out the fact that if we start with more complicated initial conditions (noise, for instance) it is not difficult to reach asymptotically stationary pulses, 2π holes, and π holes. The other localized structures were not observed for these more complex initial conditions.

As we have seen, the two sequences for ICPs and ICAs are rather different. We would like to comment on these differences as follows. Moving pulses are related to moving π holes in the following sense. If we observe the wave vector of moving pulses they have a singularity in the phase but in the part where the amplitude is practically zero. Therefore one does not notice this singularity immediately. If we start at $\mu = -0.113\,64$ with a moving pulse and we increase μ, we jump to moving π holes at $\mu = -0.113\,47$. We obtain an asymmetric hole. But now the singularity of the phase is relevant and we obtain a moving π hole. This gives a reason why moving pulses and moving π holes appear after each other as a function of μ. If we increase μ we obtain homogeneous solutions. If we reduce μ, at $\mu = -0.113\,18$ there is first a moving π hole, then we jump to moving pulses at $\mu = -0.113\,51$, and at $\mu = -0.113\,64$ to stationary pulses. We note that there is a small hysteresis in the transition from moving pulses to moving holes and vice versa.

To study the coexistence of stationary pulses, 2π holes, and π holes, we start near $\mu = \mu_1 = -0.168\,97$ with a stationary pulse. By increasing μ the system remains in such a solution until $\mu = \mu_4 = -0.1110$. If μ is increased further, a spatially homogeneous state results. When μ is decreased, the selected solution is always a stationary pulse until reaching $\mu = \mu_1$. Now we start near $\mu = \mu_5 = -0.1045$ with a 2π hole. By decreasing μ the system remains in a stationary 2π hole until reaching $\mu = \mu_3 = -0.1126$. Below this point the system jumps to a stationary pulse. If we start with a 2π hole at $\mu = \mu_3$ and we increase μ, the selected solution is a 2π hole until $\mu = \mu_5$. Above this point the system jumps to a π hole. By increasing μ the system remains in a π hole until reaching $\mu = 0$. By decreasing μ the selected solution is always a π hole until we reach $\mu = \mu_2 = -0.129$. Below this point the system jumps to a stationary pulse. Starting with a π hole at $\mu = \mu_2$ and increasing μ we remain in a π hole until $\mu = 0$. A phase diagram of stationary pulses and stationary 2π and π holes is shown in Fig. 4. From the phase diagram it is possible to see that there is a narrow range of μ, namely, $\mu_3 < \mu < \mu_4$, where stationary pulses, 2π holes, and π holes coexist. It is a remarkable fact that with a single localized initial condition (ICP or ICA) and changing μ we can jump from 2π to π holes and from there to stationary pulses.

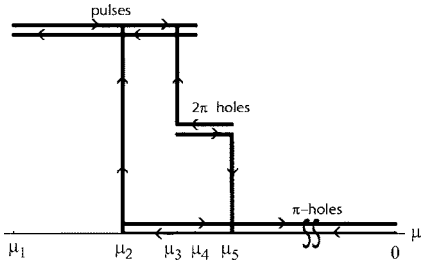

FIG. 4. Phase diagram of stationary pulses and holes. Pulses and holes coexist for $\mu_3 < \mu < \mu_4$. $\mu_1 = -0.168\,97$, $\mu_2 = -0.129$, $\mu_3 = -0.1126$, $\mu_4 = -0.1110$, $\mu_5 = -0.1045$. The μ axis is not to scale; regions of coexistence have been magnified.

Finally, we briefly show an analytic approach for 2π

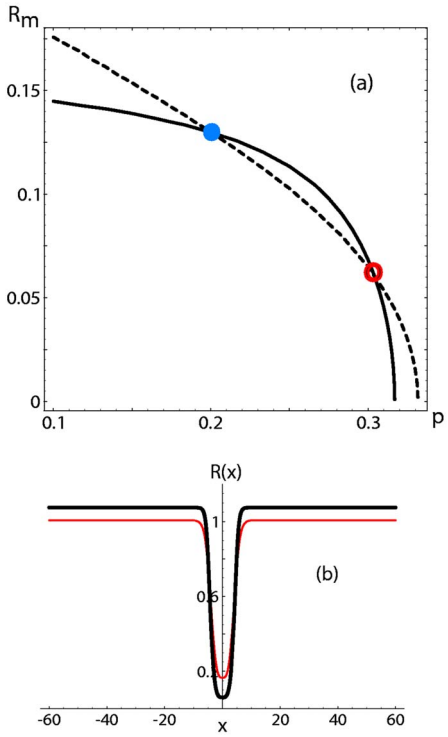

FIG. 5. (Color online) Values of the parameters are: $\mu = -0.06$, $\beta_r = 1.125$, $\beta_i = 0.48$, $\gamma_r = -0.859\,375$, and $D_r = 1$. (a) The intersection between the curves $f(p, R_m) = 0$ (continuous line) and $g(p, R_m) = 0$ (dashed line) predicts one unstable (solid circle) and one stable hole (open circle). (b) Modulus of the 2π hole. The thick line stands for the analytical prediction and the thin line for a direct numerical simulation.

holes which enables us to understand their limited existence range as shown in Fig. 4. This approach has been recently introduced only to study pulses in the one-dimensional quintic CGL equation [28]. For the sake of simplicity we consider Eq. (1) with $\gamma_i = D_i = 0$. The complex field $A(x,t)$ is supposed to be $A(x,t) = R(x)\exp\{i[\Omega t + \theta(x)]\}$. The analytic strategy to approximately calculate Ω, $R(x)$, and $\theta(x)$ consists of considering that $\theta_x(x)$ is constant ($-p$ for the left side, $+p$ for the right side) in almost all the domain (*outside the core*) except in a narrow range around the center of the hole (*core*), where $\theta_x(x)$ is considered to be a cubic function. This assumption has been inspired by numerical simulations. Replacing the above-mentioned ansatz for $A(x,t)$ in Eq. (1) and outside the core ($|x| > x_*$), where $x = x_*$ corresponds to the local maximum of the cubic function, we obtain $R_0 = \sqrt{-\beta_r - \sqrt{\beta_r^2 - 4\gamma_r(\mu - D_r p^2)}/2\gamma_r}$ (the asymptotic value of the modulus of the stationary hole), $\Omega = \beta_i R_0^2$ (the frequency), and an expression for $R(x) = R_0/\sqrt{1 + \exp\{-\Omega/D_r p(|x| - x_0)\}}$, where x_0 is a constant to be determined, which is related to the translational symmetry of Eq. (1). Inside the core ($|x| < x_*$) we assume that $R(x) = R_m + \epsilon x^2 + \delta x^4$ and $\theta_x(x) = \alpha x - \beta x^3$, where R_m is the height of the hole at $x = 0$. Replacing this ansatz in Eq. (1) we can obtain ϵ, δ, α, and β in terms of R_m, p, and the parameters of the quintic CGL equation. Imposing continuity of the amplitude $R(x)$ at $x = x_*$ we get x_0. The continuity of the first derivative of the amplitude $R(x)$ at $x = x_*$ leads us to a first relation between R_m and p: $f(p, R_m) = 0$. Using the consistency relation given in Eq. (6) in Ref. [16] we obtain a second relation between R_m and p: $g(p, R_m) = 0$. Thus we have constructed approximate expressions for $R(x)$ and $\theta(x)$ in all the domain in terms of two unknown parameters, namely, R_m and p. The existence of stationary 2π holes is related to the intersection between the curves $f(p, R_m) = 0$ and $g(p, R_m) = 0$. In Fig. 5(a) the intersection between these curves predicts one unstable and one stable hole because the appearance of 2π holes is related to a saddle-node bifurcation. For this case we plot in Fig. 5(b) the analytical predicted modulus $R(x)$ with the above-described method for the stable 2π hole (thick line). The result is in good agreement with a direct numerical simulation of Eq. (1) (thin line) (compare Ref. [29] for further details).

In conclusion, we have shown in this Communication that there are at least five different types of hole solutions for the quintic CGL equation: nonmoving π holes, nonmoving 2π holes, moving π holes, breathing moving holes, and breathing nonmoving holes. Note that both types of moving holes move either to the left or to the right to preserve the overall symmetry of the quintic CGL equation. Moreover, we have demonstrated that three different types of stationary localized solutions, namely pulses, π, and 2π holes, can arise for a fixed set of parameter values in the equation. This behavior was known so far only for a reaction-diffusion model [23]. Now that it has been shown to arise for a prototype envelope equation, we can expect the experimental observation of such a behavior with a much higher probability. Using a simple analytical method we pointed out the fact that 2π holes appear through a saddle-node bifurcation.

The simulation software DIMX developed by P. Coullet, M. Monticelli, and collaborators at the laboratory INLN in France has been used for all the numerical simulations. O.D. wishes to thank the support of FAI (Project No. ICIV-001-04) of the U. de los Andes, FONDECYT (P.1020374 and P.1050660), and Project Anillo en Ciencia y Tecnología.

[1] M. C. Cross and P. C. Hohenberg, Rev. Mod. Phys. **65**, 851 (1993).
[2] H. H. Rotermund, S. Jakubith, A. von Oertzen, and G. Ertl, Phys. Rev. Lett. **66**, 3083 (1991).
[3] K. J. Lee, W. D. McCormick, Q. Ouyang, and H. L. Swinney, Nature (London) **369**, 215 (1994).
[4] W. N. Reynolds, J. E. Pearson, and S. Ponce-Dawson, Phys. Rev. Lett. **72**, 2797 (1994).
[5] Y. Hayase and T. Ohta, Phys. Rev. Lett. **81**, 1726 (1998).
[6] P. B. Umbanhowar, F. Melo, and H. L. Swinney, Nature (London) **382**, 793 (1996).
[7] V. B. Taranenko, K. Staliunas, and C. O. Weiss, Phys. Rev. A **56**, 1582 (1997).
[8] H. R. Brand and R. J. Deissler, Physica A **204**, 87 (1994).
[9] J. Kosek and M. Marek, Phys. Rev. Lett. **74**, 2134 (1995).
[10] T. Ohta, Y. Hayase, and R. Kobayashi, Phys. Rev. E **54**, 6074 (1996).
[11] S. Koga and Y. Kuramoto, Prog. Theor. Phys. **63**, 106 (1980).
[12] V. Petrov, K. Scott, and K. Showalter, Philos. Trans. R. Soc. London, Ser. A **347**, 631 (1994).
[13] A. C. Newell and J. A. Whitehead, J. Fluid Mech. **38**, 279 (1969).
[14] H. R. Brand, P. S. Lomdahl, and A. C. Newell, Phys. Lett. A **118**, 67 (1986); , Physica D **23**, 345 (1986).
[15] I. Aranson and L. Kramer, Rev. Mod. Phys. **74**, 99 (2002).
[16] O. Thual and S. Fauve, J. Phys. (France) **49**, 503 (1988).
[17] R. J. Deissler and H. R. Brand, Phys. Rev. Lett. **72**, 478 (1994).
[18] R. J. Deissler and H. R. Brand, Phys. Lett. A **146**, 252 (1990).
[19] V. V. Afanasjev, N. Akhmediev, and J. M. Soto-Crespo, Phys. Rev. E **53**, 1931 (1996).
[20] A. Komarov, H. Leblond, and F. Sanchez, Phys. Rev. E **72**, 025604(R) (2005).
[21] K. Nozaki and N. Bekki, J. Phys. Soc. Jpn. **53**, 1581 (1984).
[22] H. Sakaguchi, Prog. Theor. Phys. **85**, 417 (1991).
[23] Y. Hayase, O. Descalzi, and H. R. Brand, Phys. Rev. E **69**, 065201(R) (2004).
[24] O. Descalzi, Y. Hayase, and H. R. Brand, Phys. Rev. E **69**, 026121 (2004).
[25] M. Mimura, M. Nagayama, H. Ikeda, and T. Ikeda, Hiroshima Math. J. **30**, 221 (2000).
[26] Moving and nonmoving holes for the quintic CGL equation have also been found by R. J. Deissler and H. R. Brand (unpublished) for completely different parameters.
[27] W. van Saarloos and P. C. Hohenberg, Phys. Rev. Lett. **64**, 749 (1990).
[28] O. Descalzi, M. Argentina, and E. Tirapegui, Phys. Rev. E **67**, 015601(R) (2003).
[29] O. Descalzi, G. Düring, and E. Tirapegui (unpublished).